Protein Kinase C Activation Promotes Microtubule Advance in Neuronal Growth Cones by Increasing Average Microtubule Growth Lifetimes✪

Nurul Kabir,* Andrew W. Schaefer,* Arash Nakhost,‡ Wayne S. Sossin,‡ and Paul Forscher*

*Yale University, New Haven, Connecticut 06520-8103; and ‡Department of Neurology and Neurosurgery, McGill University, Montreal Neurological Institute, Montreal, Quebec, Canada H3A-2B4

Abstract. We describe a novel mechanism for protein kinase C regulation of axonal microtubule invasion of growth cones. Activation of PKC by phorbol esters resulted in a rapid, robust advance of distal microtubules (MTs) into the F-actin rich peripheral domain of growth cones, where they are normally excluded. In contrast, inhibition of PKC activity by bisindolylmaleimide and related compounds had no perceptible effect on growth cone motility, but completely blocked phorbol ester effects. Significantly, MT advance occurred despite continued retrograde F-actin flow—a process that normally inhibits MT advance. Polymer assembly was necessary for PKC-mediated MT advance since it was highly sensitive to a range of antagonists at concentrations that specifically interfere with microtubule dynamics. Biochemical evidence is presented that PKC activation promotes formation of a highly dynamic MT pool. Direct assessment of microtubule dynamics and translocation using the fluorescent speckle microscopy microtubule marking technique indicates PKC activation results in a nearly twofold increase in the typical lifetime of a MT growth episode, accompanied by a 1.7-fold increase and twofold decrease in rescue and catastrophe frequencies, respectively. No significant effects on instantaneous microtubule growth, shortening, or sliding rates (in either anterograde or retrograde directions) were observed. MTs also spent a greater percentage of time undergoing retrograde transport after PKC activation, despite overall MT advance. These results suggest that regulation of MT assembly by PKC may be an important factor in determining neurite outgrowth and regrowth rates and may play a role in other cellular processes dependent on directed MT advance.

Key words: protein kinase C • microtubules • axon outgrowth • actin • growth cone

Introduction

Regulation of microtubule (MT)[1] distribution is of critical importance for many cellular processes, including directed cell motility, cell division, and establishment of cell polarity. In the developing nervous system and during nerve regeneration, axon growth depends on assembly of polarized MT arrays; however, axon guidance depends on the coordinated action of both MT assembly in the distal axon shaft and actomyosin-based lamellar motility in the neuronal growth cone (Lin et al., 1994; Tanaka and Sabry,

1995; Letourneau, 1996). In fact, dynamic interactions between MTs and the actin cytoskeleton appear to be a prerequisite for directional cell motility in general.

Neuronal growth cones (GC) have two distinct domains created by the largely discrete localization of F-actin and MTs. The central domain (C-domain) has a high density of MTs and organelles and is separated from the F-actin–rich peripheral domain (P-domain) by an interface referred to as the transition (T) zone. F-actin–based motility in the P-domain has been shown to result from constitutive plus-end–directed actin assembly into networks and filopodia at the leading edge and the concurrent action of myosin motors capable of translocating actin networks away from the leading edge centripetally towards the central domain—a process referred to as "retrograde F-actin flow" (Forscher and Smith, 1988; Mitchison and Kirschner, 1988; Cramer et al., 1994; Tanaka and Sabry, 1995; Lin et al., 1996; Mitchison and Cramer, 1996). Several lines of evidence suggest that F-actin networks and retrograde flow pose a barrier to MT advance and MT-dependent organelle transport into the P-domain. For example, clear-

---

✪The online version of this paper contains supplemental material.

Drs. Kabir and Schaefer contributed equally to this work and should be considered co-first authors.

Address correspondence to Paul Forscher, Dept. Molecular, Cellular and Developmental Biology, KBT338, Yale University, P.O. Box 208103, New Haven, CT 06520-8103. Tel.: (203) 432-6344. Fax: (203) 432-8999 or (203) 432-6161. E-mail: paul.forscher@yale.edu

[1]*Abbreviations used in this paper:* Bis, bisindolylmaleimide; FSM, fluorescent speckle microscopy; GC, growth cone; MAP, microtubule-associated protein; MT, microtubules; OAG, 1-oleoyl-2-acetyl-*sn*-glycerol; P (or C)-domain, peripheral (or central) domain; PDBu, phorbol dibutyrate; T zone, transition zone; TPA, 12-*O*-tetradecanoylphorbol-13-acetate; VE-DIC, video-enhanced differential interference microscopy.

ance of F-actin networks subsequent to cytochalasin exposure results in rapid MT and organelle advance into the P-domain (Forscher and Smith, 1988; Waterman-Storer and Salmon, 1997); furthermore, recent evidence suggests that retrograde F-actin flow can translocate MTs from peripheral F-actin domains and decreases MT plus-end assembly rates in newt lung cells (Waterman-Storer and Salmon, 1997). Finally, MT advance and retrograde flow are inversely correlated during GC interactions either with native target substrates (Lin and Forscher, 1995) or Ig CAM-coated bead substrates (Letourneau et al., 1987; Lin et al., 1996; Suter et al., 1998).

Abundant and long-standing evidence implicates protein kinase C as a regulator of cytoskeletal organization and neurite outgrowth. For example, treatment with activators of PKC such as phorbol dibutyrate (PDBu) or 12-O-tetradecanoylphorbol-13-acetate (TPA) result in neurite extension in embryonic ganglia explants (Hsu et al., 1989), neuroblastoma cells (Fagerstrom et al., 1996), and NGF-treated PC12 cells (Hundle et al., 1995), as well as changes in filopodial and lamellipodial protrusions in rat cerebral neurons and affect MT distribution in SH-SY5Y neuroblastoma growth cones (Rosner and Fischer, 1996). Conversely, PKC inhibition can result in reduced rates of neurite outgrowth as well as dramatic changes in growth cone structure, sometimes referred to as "GC collapse" (Bixby, 1989). Given that several well-known PKC substrates (e.g., GAP-43 and MARCKS) interact with and affect F-actin, previous studies have typically invoked PKC regulation of F-actin structure and motility to explain these effects (Meiri et al., 1988; Hartwig et al., 1992; He et al., 1997; Dent and Meiri, 1998). Microtubule-associated proteins (MAPs) such as MAP1B and MAP2 and Tau (Gordon-Weeks, 1993; Liu et al., 1999) are also abundant PKC substrates in axons, and phosphorylation by PKC tends to inhibit their MT assembly-promoting activity (Mori et al., 1991); however, the mechanism by which MAP or tau phosphorylation promotes increased neurite outgrowth appears to involve complex interactions between multiple signaling pathways (Goold et al., 1999) and is not well understood. In this report, we describe a novel mechanism by which PKC regulates MT advance by controlling assembly of a highly dynamic pool of MTs normally residing in the T zone. PKC activation promotes MT invasion deep into the P-domain, where MTs are rarely found under control conditions by a process that increases the lifetime of MT growth events.

Materials and Methods

Cell Culture, Chemicals and Video Microscopy

Primary culture of Aplysia bag cell neurons and video-enhanced differential interference microscopy (VE-DIC) was performed as previously described (Forscher et al., 1987). Appropriate stock solutions of chelerythrine chloride, calphostin C, bisindolylmaleimide 1, Gö-6976, Ro32-0432, PDBu, 4-α-phorbol, 1-oleoyl-2-acetyl-*sn*-glycerol (OAG), nocodazole, taxol, vinblastine (Calbiochem) and other drugs were prepared in DMSO and stored in −20°C. Fresh dilutions were made before each experiment in artificial sea water containing 2–3 mg/ml BSA as an amphipathic vehicle to aid drug solubilization in the high salt medium. PDBu was used rather than phorbol-12-myristate-13-acetate (PMA or TPA) since it is better characterized in Aplysia (Sossin and Schwartz, 1994) and there was no observable difference between the actions of PDBu and PMA. We mea-

sured the absorption profile of the various PKC activators and inhibitors (data not shown) and have found that most of these PKC-related drugs absorb light in the green range. When VE-DIC was performed with white or green light, phototoxic effects were greater in the presence of these drugs. Therefore, VE-DIC was performed with 650–750-nm light except for calphostin C, since this compound is actually activated by 450–650-nm light (Gopalakrishna et al., 1992).

Immunocytochemistry

After each pharmacological experiment, cells were fixed and stained for F-actin and microtubules as described (Forscher and Smith, 1988), with the following modifications. F-actin was labeled with alexa 568 or 594 phalloidin. For MTs, alexa 488–labeled secondary antibody was used. The alexa dyes (Molecular Probes) were brighter, more photostable, and gave better separation of emission spectra relative to FITC and rhodamine.

Retrograde Flow Measurements

Retrograde flow of F-actin in lamellipodia was measured using Con-A–coated or polyethylenimine-coated 500-nm silica beads (Bangs Laboratories) in the presence of 3 mg/ml BSA. Verification of beads as F-actin markers in this system, ionizing radiation–laser trapping and measurement of bead displacement were as previously described (Lin and Forscher, 1995).

Analysis of MT Invasion of P-Domain F-Actin

MT density in the P-domain was measured by counting the number of microtubules spanning 75% of the P-domain as defined by distal and proximal borders of F-actin bundle labeling (see Fig. 3). Data was normalized between growth cones by GC area and expressed as the number of MT/100 μm^2; i.e., MT density.

Biochemical Experiments on Nocodazole-sensitive Triton X-100 Insoluble Fraction

Handling of Aplysia, dissection of abdominal ganglion, Western blots, and quantification of immunoblots were as previously described (Nakhost et al., 1998). In Aplysia, the pleural-pedal ganglia are symmetrically paired on either side of the animal. In all experiments, the ganglion on one side of the animal was used as a control for the corresponding one on the other side. The ganglia were desheathed to facilitate penetration of pharmacological agents and transferred to resting medium (the same as dissecting medium, but with 460 mM NaCl, 11 mM $CaCl_2$, 55 mM $MgCl_2$; as described by Sossin and Schwartz, 1994). The ganglia were incubated in either 1 μM 4α-PDBu (control) or 1 μM 4β-PDBu (experimental) for 1 h at 15°C (physiological temperature of Aplysia). The ganglia were then washed twice with microtubule stabilization buffer (0.1 M MES, 1 mM EGTA, 0.5 mM $MgCl_2$) containing 1 mM GTP and 10% glycerol (RGG buffer) and homogenized in 120 μl of RGG buffer containing protease inhibitors (20 μg/ml aprotinin, 5 mM benzamidine, and 0.1 mM leupeptin) and 1% Triton X-100. The samples were centrifuged at 15°C for 1 min at 800 g to remove any unhomogenized debris. The resulting homogenates (100 μl) were centrifuged at 100,000 g for 30 min. Supernatants were isolated and added to 20 μl of sample buffer. Pellets were either resuspended in sample buffer or resuspended in 120 μl RGG plus protease inhibitors and divided into two 50-μl fractions. Subsequently, one fraction from each of the experimental and control ganglia was incubated with 100 nM nocodazole (in RGG plus protease inhibitors), while the other fraction was incubated with vehicle. The samples were incubated at 15°C for 15 min, and then centrifuged at 15°C for 30 min at 94,000 g. The supernatants were removed and added to 12 μl of sample buffer. The pellets were resuspended in 72 μl of sample buffer. The samples were loaded onto 9% SDS-polyacrylamide gels and analyzed by immunoblotting with antitubulin antibody (clone DM 1A; Sigma-Aldrich).

Microtubule Dynamics and Multimode Microscopy

Microtubule dynamics were assessed using the recently described fluorescent speckle microscopy (FSM) technique (described in Waterman-Storer, 1998; Waterman-Storer and Salmon, 1998). Neurons were injected with ∼1 mg/ml rhodamine-labeled tubulin (Cytoskeleton Inc.) in injection buffer (100 mM Pipes, 1 mM $MgCl_2$, 1 mM EGTA) and allowed to recover for ∼60 min in L15–artificial sea water medium (Forscher et al., 1987) supplemented with 3 mg/ml BSA. Under these conditions, MT

speckles could be clearly discerned in distal axonal regions and used as fiduciary marks for assessment of MT growth, shrinkage, pause, and translocation rates and lifetimes. MT image sequences were obtained using a Nikon Eclipse TE300 microscope equipped with a Photometrics Quantix 57 back-illuminated frame transfer cooled CCD camera and filter wheels (Ludl Inc.) for changing both excitation and emission wavelengths and rapid switching between fluorescence and DIC imaging modes. Metamorph control software (Universal Imaging Corp.) was used for instrument control and image analysis. Images were recorded every 10 s using 300–500-ms integration times for fluorescent MTs and 50-ms for DIC. Contrast of the speckles was enhanced by processing the fluorescent images sequentially with the following spatial filters: unsharp mask, low pass, laplace edge enhancement, and a final low pass. For DIC-fluorescent overlays, a threshold look-up table was applied to MT images before combining with the DIC image to clear low level background noise.

Online Supplemental Material

Representative examples of microtubule dynamics and the structural response of the growth cone to PKC activation are viewable as Quicktime movies. In the single-channel microtubules dynamics examples, the open arrow follows the distal MT end and the closed arrow is an internal reference mark. The other examples are dual channel DIC-microtubule movies with MTs pseudocolored in green. All movies are labeled according to the corresponding figure except the example of MT buckling. Online supplemental materials can be found at http://www.jcb.org/cgi/ content/full/152/5/1033/DC1.

Results

PKC Activation Results in Microtubule Invasion of the P-Domain

Fig. 1 illustrates the typical C-, P-, and T-domain structures of a growth cone under control conditions (see Forscher and Smith, 1988), note the relatively low density of MTs penetrating into the P-domain. Fig. 2 shows the effects of PKC activation on growth cone structure and the underlying MT and actin cytoskeleton. PKC activation

with 1 μM PDBu (Sossin and Schwartz, 1994) resulted in relatively minor acute (~5 min) morphological effects at the level of VE-DIC imaging, with the exception of rapid attenuation of T zone ruffling (not shown). After 30 min in PDBu (Fig. 2 B), C-domain organelles appeared to have advanced slightly (A and B, dotted line) and attenuation of ruffling persisted. Visualization of F-actin (Fig. 2 C) after 30 min in 1 μM PDBu revealed an intact P-domain F-actin structure, including well-defined F-actin bundles; however, F-actin hotspots corresponding to ruffling in the T zone were notably absent (Fig. 2 C). Surprisingly, immunofluorescent visualization of β-tubulin revealed that a striking advance of MTs into the F-actin–rich P-domain had occurred during PDBu treatment (Fig. 2 D). This robust advance or "invasion" of the MTs into the P-domain was unexpected, occurred as early as 5 min after 1 μM PDBu application, and with doses of PDBu as low as 10 nM for 30 min (data not shown). Invading microtubules were mostly unbundled, straight, and, in many cases, ran along or near F-actin cables (Fig. 2, C and D, arrowheads; see also Fig. 4, C and D). Treatment with 1 μM 4-α-phorbol (Fig. 2, I–L), an inactive phorbol-ester analogue, had no observable effects on growth cone motility or structure (Fig. 2, E–H).

To determine whether these effects were due to PKC activation, we preincubated cells with 10 μM bisindolylmaleimide 1 (Bis 1), a specific PKC inhibitor that interacts with the ATP binding site, for 15 min, and then added 1 μM PDBu and 10 μM Bis 1 for an additional 30 min. Essentially all the morphological (Fig. 2, I and J) and cytoskeletal (K and L) changes observed during PDBu treatment were absent in the presence of Bis 1; note that only a few MTs invade the P-domain (Fig. 2 L) and actin-based ruffling in the T zone is still clearly present (J and K). In
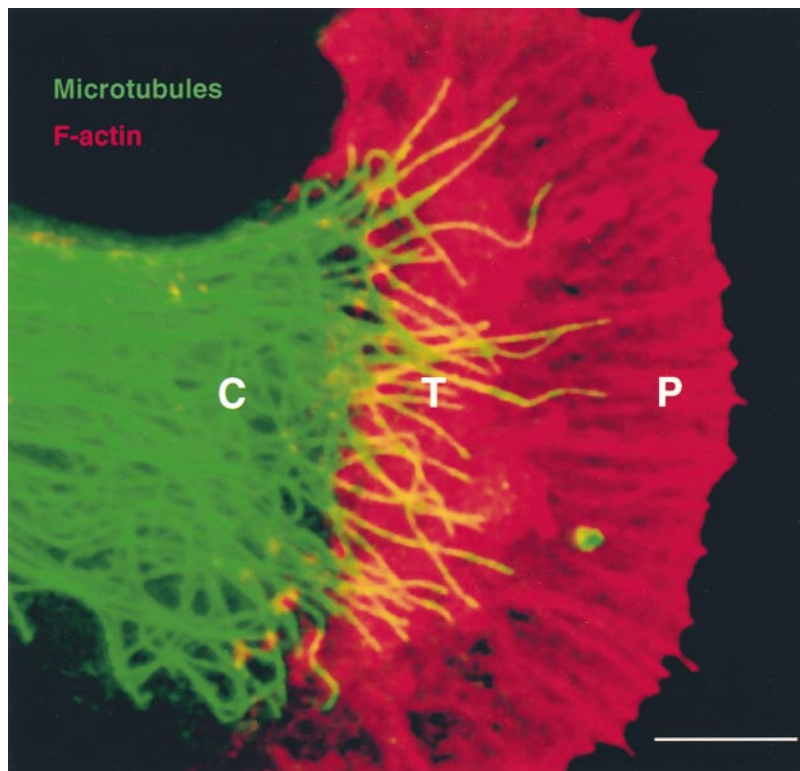

Figure 1. F-actin and MT distribution in Aplysia bag cell neuron growth cone. The growth cones of Aplysia bag cells are characterized by a P-domain rich in F-actin and a C-domain rich in MTs. The T zone is characterized by ruffles containing both F-actin and MTs. Note that although under control conditions some microtubules invade the P-domain F-actin, almost none reach near the leading edge (75% threshold). Scale bar, 5 μm.
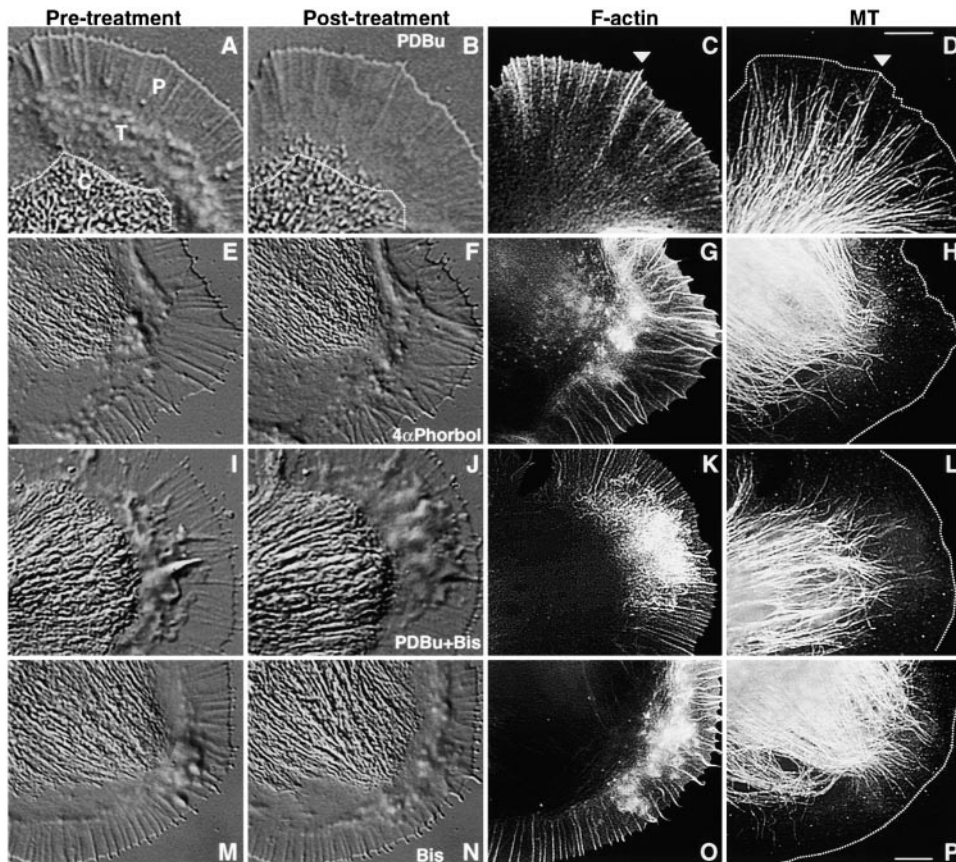
Pre-treatment	Post-treatment	F-actin	MT

Figure 2. Activation of PKC results in MT invasion of the P-domain. Growth cones were treated with PDBu (A–D), 4-α-phorbol (E–H), PDBu plus Bis (I–L), or Bis alone (M–P) for 30 min, and then fixed and stained for F-actin (C, G, K, and O) and MTs (D, H, L, and P). 30 min after treatment with 1 μM PDBu, there was slight C-domain advance (A and B, dotted lines) and attenuated ruffling (B). P-domain F-actin structure (C) was relatively unperturbed; whereas, MT labeling (D) reveals a striking advance into the P-domain. PDBu responses were absent after exposure to inactive phorbol ester analogue (1 μM 4-α-phorbol, E–H) or a 15-min pretreatment with the PKC inhibitor, 10 μM Bis 1 (I–L). Exposure to 10 μM Bis 1 alone (M–P) was also without effect. White dotted lines (D, H, L, and P) demarcate leading edge. Arrowheads (C and D) indicate MT advance along F-actin cables. Scale bars, 5 μm (A–D, bar in D; E–P, bar in P).

addition, treatment with 10 μM Bis 1 alone for 45 min had little or no effect on growth-cone motility or cytoskeletal structure (Fig. 2, M–P). In summary, Bis 1 did not affect basal GC motility, morphology, or cytoskeletal structure, but completely inhibited PDBu-mediated changes in these attributes.

Microtubule invasion levels (shown in Fig. 3) were quantified by determining the density of MTs spanning 75% of the P-domain, the latter defined by F-actin labeling (see Materials and Methods; Fig. 3, inset). Under control conditions, there were 0.9 ± 0.2 MT/100 μm^2. After 30 min of 1 μM PDBu treatment, MT density increased to 6.7 ± 1.2 MT/100 μm^2. In addition, chronic activation of PKC with lower doses of PDBu (e.g., 40 nM for 16 h) had similar effects on MT distribution (data not shown). In contrast, after inhibition of PKC with 10 μM Bis 1 for 45 min, there were 0.7 ± 0.1 MT/100 μm^2 (Fig. 3); i.e., similar to control levels. Importantly, PDBu did not increase MT density above control levels in the presence of 10 μM Bis 1. Treatment with 1 μM 4-α-phorbol for 30 min also had no effect on the number of MTs invading the growth cone. Treatment with 10 μM OAG resulted in a less robust but statistically significant advance of MTs (3.1 ± 0.8 MT/100 μm^2 crossed the 75% threshold), as expected from its lower potency relative to PDBu. In summary, activation of PKC was found to significantly increase the density of MTs found in the distal P-domain. This effect was not present with inactive phorbolester analogues and was completely prevented by specific PKC inhibitors such as Bis1 (Figs. 2 and 3) as well as 10 μM Gö-6976 or 10 μM Ro32-0432 (data not shown).

PDBu-mediated MT Extension Does Not Result from a Decrease in Retrograde F-Actin Flow

There is evidence that P-domain F-actin and the process of retrograde flow itself inhibits MT advance and plus-end assembly (Forscher and Smith, 1988; Waterman-Storer and Salmon, 1997). Thus, a possible mechanism for PDBu-mediated MT advance was a change in retrograde F-actin flow. Using a laser trap–assisted flow-coupled bead assay to quantitatively assess F-actin flow rates as previously described (Lin and Forscher, 1995), we found no evidence for a decrease in retrograde flow of F-actin in growth cones subsequent to PDBu treatment. Fig. 4 (A and B) illustrates an example of a retrograde flow assay before and after treatment with 1 μM PDBu for 30 min. Note that flow actually increased slightly after 30 min in PDBu (6.2 ± 1.9 μm/min) compared with controls (4.9 ± 1.5 μm/min) in this experiment; however, this increase was not significant over all experiments done ($n = 6$; $7.9 \pm 7.0\%$ increase in retrograde flow after PDBu). The presence of intact F-actin structure as well as MT extension was verified by post-experiment fixation and MT immunofluorescence, note that MT advance often occurred along lines defined by F-actin cables (Fig. 4, C and D, arrowheads). These results indicate that PKC-mediated MT extension is not due to attenuation of retrograde flow. In addition, experiments to investigate changes in the gel exclusion properties of the P-domain using microinjected FITC-dextrans indicate that there is little change in the functional pore size of the P-domain after PDBu treatment, suggesting that simple alteration of the physical properties of the cytomatrix are
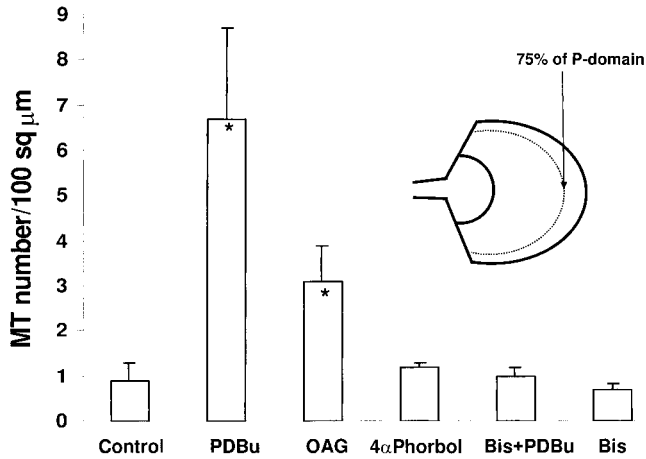
Figure 3. Quantification of the MT invasion data. Bag cells were treated with various drugs as indicated for 30 min, and then fixed and stained for MTs and F-actin. MT density was calculated by counting the number of MTs crossing >75% of the P-domain and normalizing by area. *$P < 0.001$, Student's t test.

not likely to account for the observed effects (our unpublished observations, see Discussion).

PDBu-mediated Microtubule Extension Depends on Microtubule Assembly

To address whether MT assembly was involved, PDBu effects were assessed under conditions where MT dynamics were damped with low concentrations of nocodazole or taxol. We specifically chose conditions previously shown to inhibit plus-end MT assembly without significantly reducing polymer mass (Bamburg et al., 1986; Tanaka et al.,

1995; Rochlin et al., 1996) or, alternatively, to stabilize MTs (Letourneau et al., 1987; Jordan and Wilson, 1998b). Fig. 5, A–D, illustrates the effects of exposure to 100 nM nocodazole on growth-cone structure and the cytoskeleton. Similar effects were observed after exposure to 1 μM taxol (Fig. 5, E–H). Note retraction of the C-domain (Fig. 5, A and B, E and F, dotted lines) and depletion of MTs from the T zone (D and H) observed after a 30-min exposure to either nocodazole or taxol. Interestingly, despite essentially complete separation of C and P cytoplasmic domains and the underlying microtubule retraction, retrograde F-actin flow continued unabated (data not shown) and P-domain F-actin remained relatively unperturbed in both cases. These results suggest that dynamic MTs are not necessary for maintenance of retrograde F-actin flow, but are a prerequisite for MT advance out of the C-domain into more distal regions. In agreement with these results, persistent growth-cone motility and absence of P-domain MTs were reported after treatment of *Xenopus* neurons with nanomolar levels of vinblastine (Tanaka et al., 1995). Note also the relatively high level of diffuse tubulin labeling in nocodazole (Fig. 5 D) when compared with taxol-treated growth cones (Fig. 5 H), where diffuse tubulin labeling is low, as expected from the decrease in critical tubulin concentration.

We then tested whether PDBu-mediated invasion requires dynamic MTs by treating growth cones with taxol or nocodazole at or below the levels illustrated above. In the absence of PDBu, all of the MT drugs examined (including vinblastine and colchicine; data not shown) decreased the density of MTs in the T zones and P-domains (as in Fig. 5, A–H) in a dose-dependent manner. The effects of nocodazole were examined quantitatively since this drug was found to be highly potent and its mode of action is re-
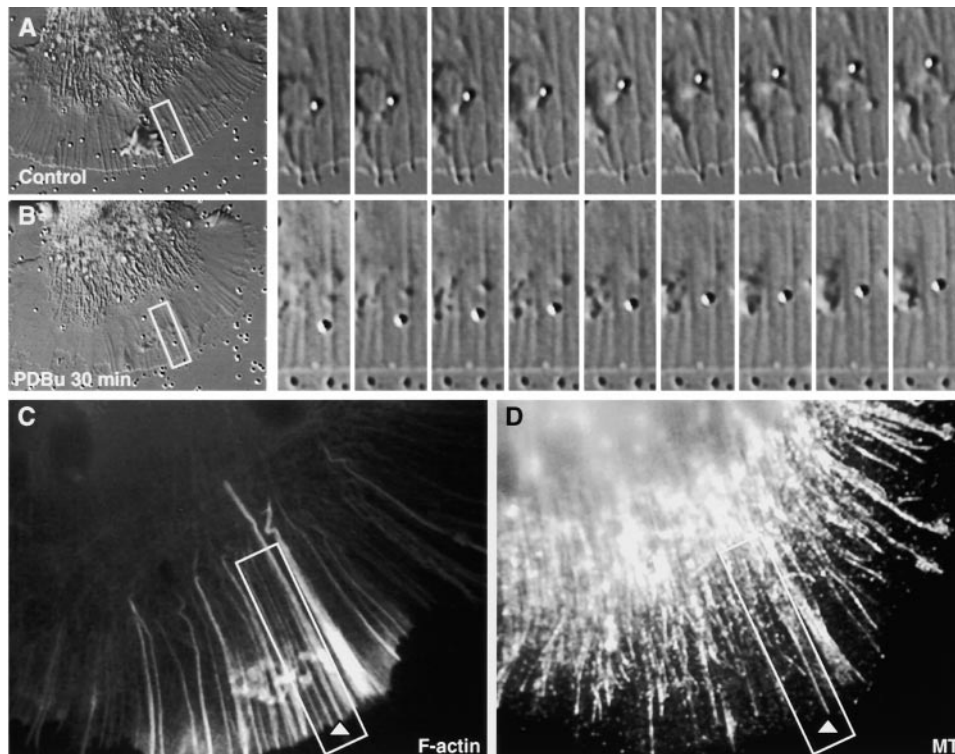

Figure 4. Retrograde flow of F-actin is not significantly reduced during PDBu-mediated MT invasion of the P-domain F-actin. (A) polyethylenimine (PE)-coated 500-nM beads were used to measure retrograde flow. Sequence of images at 5-s interval. (B) PE-coated beads undergo continued retrograde flow after a 30-min treatment with 1 μM PDBu. The cell was then fixed and stained for F-actin (C) and MT (D). Note that MT advance into P-domain F-actin has occurred in the region of the bead movement (D, box), and F-actin structure is not significantly altered (C). Arrowheads (C and D) indicate MT advance along F-actin cables.
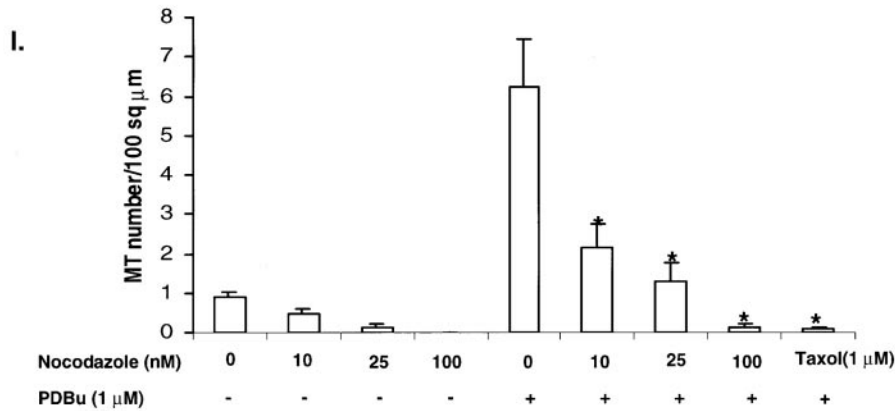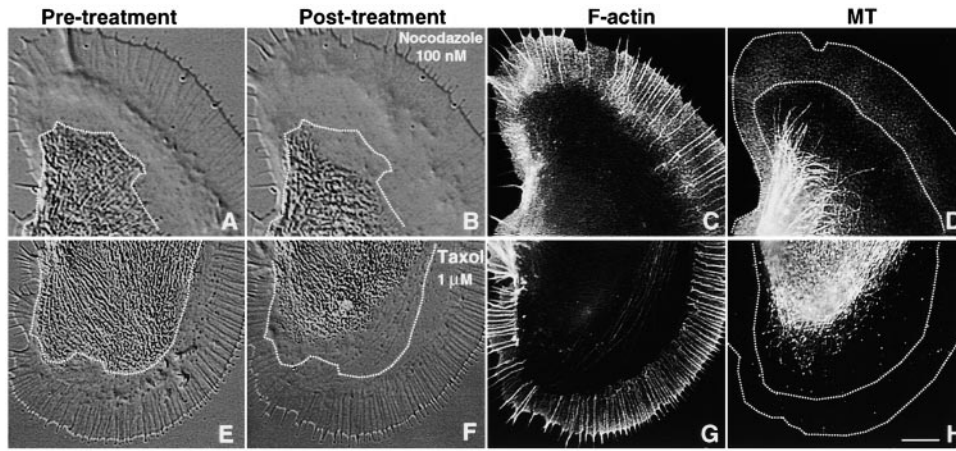
Pre-treatment	Post-treatment	F-actin	MT

Figure 5. MT dynamics are necessary for PDBu-mediated MT invasion of the P-domain. (A–H) Effects of a 30-min treatment with 100 nM nocodazole (A–D) or 1 μM taxol (E–H) on structure, F-actin, and MTs. Note central domain retraction in both nocodazole (dotted lines, A and B, and taxol, E and F, and accompanying MT retraction, D and H (dotted line indicates proximal P-domain boundary). C- and P-domains are clearly separated after either treatment, yet P-domain actin structure remains intact (C and G) at the 30-min time point. (I) Low doses of nocodazole or taxol inhibit PDBu-mediated MT invasion of the P-domain. Growth cones were treated for 30 min with the doses of nocodazole indicated, and then 1 μM PDBu + Nocodazole for an additional 30 min. Cells were fixed, stained for MTs and F-actin, and MT density was then assessed as in Fig 3. Note that 10 nM nocodazole inhibited the PDBu-mediated MT invasion of the P-domain. *$P < 0.001$, Student's t test. Scale bar, 5 μm.

ported to be somewhat less complex and more readily reversible than the others (Jordan and Wilson, 1998b). Cells were treated with 0, 10, 25, or 100 nM nocodazole ± PDBu and P-domain MT density was assessed (Fig. 5 I). In the absence of PDBu, distal axonal MT's (i.e., in the T zone and P-domain) were highly sensitive to nocodazole, as previously reported (Bamburg et al., 1986), with inhibitory effects at doses >10 nM. In the presence of 1 μM PDBu, clear and highly significant ($P < 0.001$) inhibitory effects on MT extension were observed at nocodazole doses as
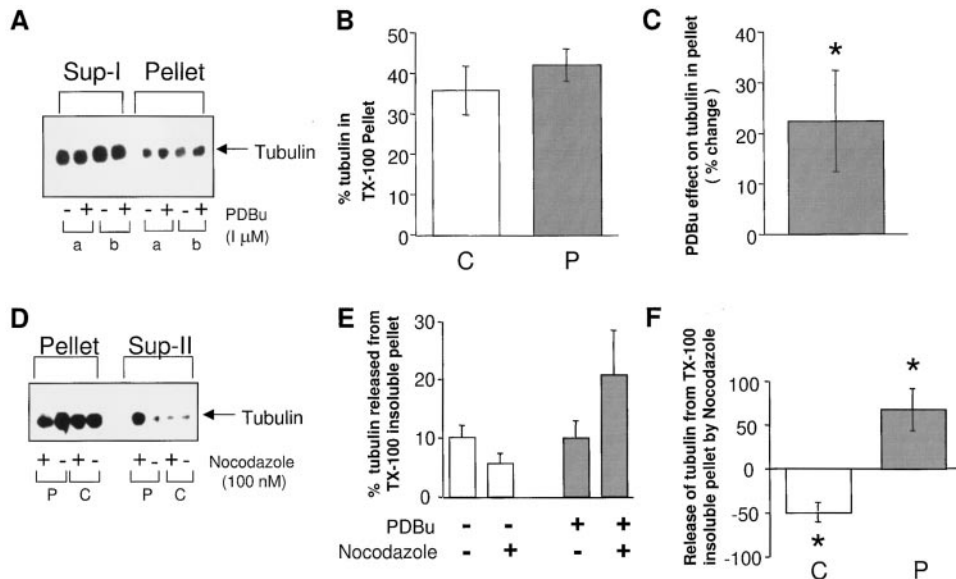

Figure 6. PDBu results in increased assembly of nocodazole-sensitive microtubules. (A) Paired pleural-pedal ganglia were incubated in either 1 μM PDBu (+) or 1 μM of the inactive isomer 4-alpha PDBu (−), homogenized in microtubules stabilization buffer and free tubulin separated from microtubules at 100,000 g. Equal proportions of supernatant (Sup-I) and pellet were separated on 9% SDS-PAGE gels, transferred to nitrocellulose, and immunoblotted for tubulin. Results are shown for two animals (a and b). Results from five experiments are quantitated in B (unpaired results for percentage of tubulin in pellet) and C (percent change in tubulin in PDBu-treated ganglia compared with untreated control). $P < 0.05$, paired Student's t test. (D) Tx-100–insoluble pellets from control (C) or PDBu (P)-treated ganglia were incubated in 100 nM nocodazole in stabilization buffer (+) or stabilization buffer alone (−). The microtubules were resedimented and equal proportions of the released supernatant (Sup-II) and pellet were separated on 9% SDS-PAGE gels, transferred to nitrocellulose, and immunoblotted for tubulin. Results from five experiments are quantified in (E) unpaired results for percentage of tubulin released from pellet and (F) effect of nocodazole on release of tubulin. *$P < 0.05$, paired Student's t test.
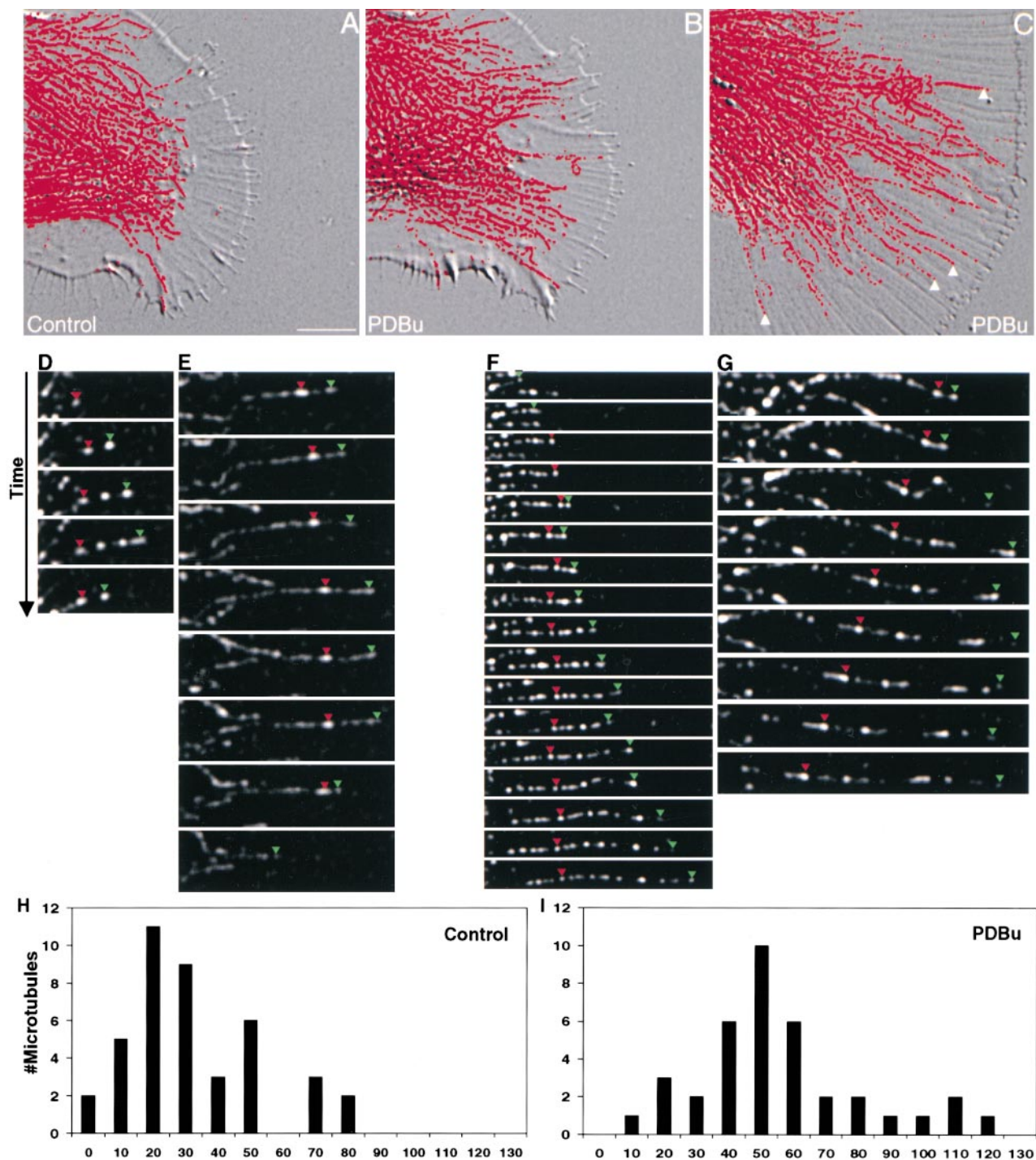
Figure 7. PDBu increases MT growth lifetimes. (A) DIC-MT (MT pseudocolored red) overlay showing the distribution of MTs in a living control growth cone. (B) Invasion of MTs into the periphery of the same growth cone after 30 min in 500 nM PDBu. (C) Another example of a PDBu-treated growth cone showing codistribution of MTs and actin cables (arrowheads). Scale bar, 10 μm. (D–G) Time lapse montages (10-s intervals, box lengths: D, 8.3 μm; E, 13.3 μm) of MT behavior visualized by FSM under control conditions (D and E) and after PDBu exposure (F and G). Red triangles indicate the same fluorescent speckle over time; green triangles mark speckle at distal MT end. Note the period of rapid MT growth (green arrowheads) accompanied by retrograde translocation (red arrowheads) in G (box lengths: F, 17.3 μm; G, 18.5 μm). (H–I) MT growth lifetime histograms under control conditions (H) and after PDBu treatment (I). Bin 0 indicates MTs that were paused throughout the 240-s sampling interval used to generate histograms. Note that the sampling interval was 10 s; therefore, there is some uncertainty in the lifetime of MTs in the 10 s bin; i.e., lifetimes ≥10 to <20 s.

low as 10 nM and inhibition of the PDBu response was essentially complete in 100 nM nocodazole. The extreme nocodazole sensitivity observed after PDBu treatment suggests that MTs assembled subsequent to PKC activation may be highly dynamic (Jordan et al., 1992; Rochlin et al., 1996; Challacombe et al., 1997; Jordan and Wilson, 1998a). Low doses of vinblastine or taxol (Fig. 5 I) also inhibited PDBu-mediated MT advance. In summary, these results indicate that MT assembly is a necessary component of PDBu-mediated MT advance.

Table I. Microtubule Dynamic Parameters

	Growth	Shortening	Anterograde translocation	Retrograde translocation	Catastrophe frequency	Rescue frequency
	μm/min				*min⁻¹*	
Control	7.14 ± 0.33	-11.75 ± 0.55	5.35 ± 0.5	-4.09 ± 0.39	1.21 Total 0.98 Peripheral*	1.44 Total 1.88 Peripheral*
PDBu	7.75 ± 0.38	-14.65 ± 1.71	5.00 ± 0.46	-4.39 ± 0.34	0.62 Total 0.58 Peripheral*	2.42 Total 2.37 Peripheral*

*Catastrophe and rescue frequencies calculated for MTs persisting in the peripheral domain for at least 90 s of total elapsed time.

PDBu Treatment Increases the Nocodazole-sensitive Tubulin Pool

To assess PDBu effects on microtubule assembly using an independent methodology, biochemical experiments were performed on Aplysia central nervous system tissue. Detecting changes in soluble tubulin biochemically in the face of high baseline levels was not possible due to signal-to-noise problems. However, given the apparent high sensitivity of newly assembled MTs to nocodazole, we tested whether PDBu would increase the nocodazole-sensitive MT pool as an alternative approach. Experiments were performed on paired nervous systems from the same animal treated with either 1 μM PDBu or 1 μM of the inactive isomer 4-α phorbol. Ganglia were lysed in microtubule stabilization buffer, and free tubulin and microtubules were separated by sedimentation. We found a small but significant increase in the percentage of tubulin found in the pellet after PDBu treatment (Fig. 6, A–C). To determine whether this increase was due to assembly of nocodazole-sensitive microtubules, we assessed the amount of tubulin released from pellets by 100 nM nocodazole. Nocodazole induced a significant increase in the amount of tubulin released from pellets prepared from PDBu-treated ganglia (Fig. 6, D–F); furthermore, the amount of tubulin released by nocodazole approximately matched the increase in tubulin sedimented after PDBu (Fig. 6 C). Paradoxically, treatment with low doses of nocodazole alone resulted in a small decrease in the amount of tubulin released from the Triton-insoluble pellet (Fig. 6, D and E). Similar effects have been reported in *Xenopus* extract preparations (Canman and Bement, 1997); however, this effect is not well understood and moreover was not observed in the presence of PDBu. Overall, these biochemical results are consistent with PDBu increasing assembly of a dynamic (i.e., nocodazole-sensitive) pool of microtubules and support our in vivo findings that PDBu results in nocodazole-sensitive MT advance.

MT Advance Results from Increased MT Growth Lifetimes after PKC Activation

To directly address the mechanism of the PKC effects described above, we assessed microtubule dynamics before and after treatment with PDBu using FSM. This relatively new microtubule marking technique (Waterman-Storer et al., 1998; Waterman-Storer and Salmon, 1998) permits rapid assessment of the critical dynamic parameters of MT behavior, including assembly, disassembly, and translocation (sliding) rates as well as MT lifetimes in each state. Fig. 7 shows DIC-MT overlays illustrating the distribution of MTs before (A) and after (B) PDBu exposure with respect to growth-cone structure. Fig. 7 C is another growth cone in PDBu illustrating extended undbundled MTs typically observed after PDBu treatment. Note the spatial overlap between MTs and actin cables that extend into filopodia (Fig. 7 C, arrowheads), as observed in fixed cells (compare Fig. 4, C and D). Representative MT behavior under control conditions is illustrated in the time-lapse image montages shown in Fig. 7, D and E. MTs underwent stochastic bursts of growth and shortening (green arrowheads indicate the penultimate plus-end speckle) superimposed on relatively short MT translocations in both directions, as indicated by speckles maintained within the body of MTs over time (red arrowheads). Under control conditions, microtubule growth, shrinkage, and sliding activity occurred within the transition zone with only occasional MT excursions into the P-domain. In contrast, after PDBu exposure, MTs often extended deep into the P-domain and occasionally reached the leading edge of the growth cone. This extension resulted from an increase in MT growth lifetimes as shown in the MT growth lifetime histograms in Fig. 7, H and I, under control conditions and after PDBu treatment. Note the presence of MT growth lifetimes in excess of 80 s in PDBu (Fig 7 I) and the nearly twofold increase in mean MT growth lifetime (Fig. 8 A). An example of a prolonged MT growth lifetime in PDBu is shown in Fig. 7 F. The increase in growth lifetimes in PDBu was accompanied by a 1.7-fold increase in the MT rescue frequency and an approximately twofold decrease in catastrophe frequency (Table I). Rates of MT growth and shortening increased slightly after PDBu treatment (Table I), but these changes were not statistically significant. Anterograde and retrograde translocation rates remained unchanged (Table I).

Interestingly, after PDBu treatment, MTs penetrating the P-domain sometimes underwent prolonged periods of retrograde translocation, apparently in conjunction with retrograde F-actin flow. An example of this phenomenon is illustrated in Fig. 7 G, where a MT continuously translocates in the retrograde direction (red marks) while still growing at a rate that matched or exceeded the rate of retrograde transport. This resulted in the distal tip of the MT maintaining its position near the leading edge despite the opposing retrograde F-actin flow. To analyze the contribution of MT translocation in the observed effects, the percentage of time MTs spent moving in the anterograde or retrograde direction or in a nonmoving state was assessed under control conditions and after PDBu treatment. We found MTs spent significantly more time undergoing retrograde movement after PDBu treatment and a proportional decrease in the amount of time MTs were not moving (Fig. 8 B). It should be emphasized that net MT extension occurred despite the increase in retrograde MT
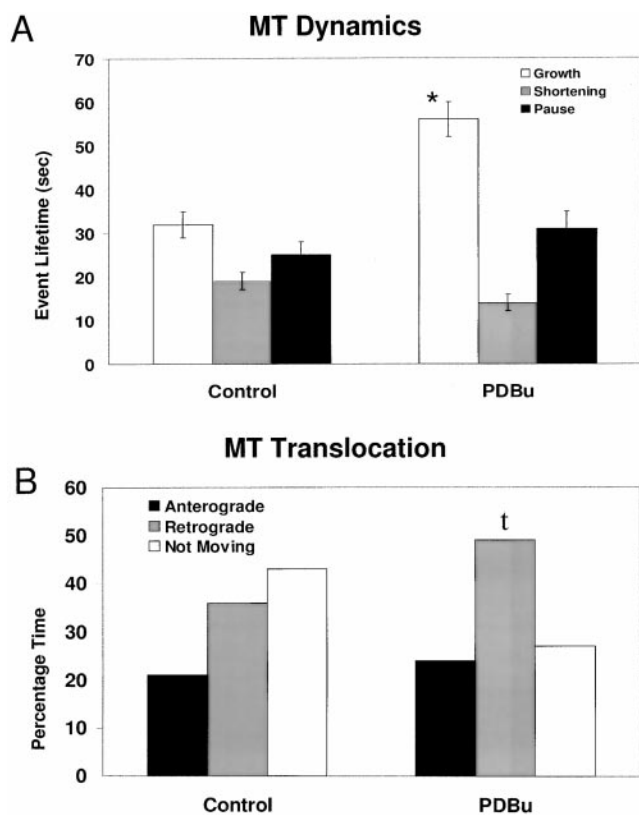
A

MT Dynamics

B

MT Translocation

Figure 8. Quantification of MT assembly versus translocation dynamics. Data compiled from four control and four PDBu-treated growth cones. DIC and fluorescence images were collected at 10-s intervals for 240 s. A total of 41 control and 37 PDBu MTs were analyzed. (A) PDBu treatment significantly increases the length of time MTs spend in growth phase, *$P < 0.00004$, paired student's t test. (B) Percentage of time MTs undergo retrograde or anterograde translocation and time not moving under control conditions and after PDBu. The actual time MTs undergo retrograde translocation increases significantly ($P < 0.01$, paired Student's t test) in control (27 ± 3 s) versus PDBu treatment (50 ± 6 s).

translocation described here. PDBu had insignificant effects on anterograde MT movements.

Discussion

PDBu Stimulated PKC Activity and Growth-Cone Structure

The effects of PDBu on MTs appear to be specifically due to PKC-regulated events since multiple activators such as PDBu, TPA, or OAG had similar MT assembly-promoting effects that could be completely blocked by specific PKC inhibitors and not observed with the inactive PDBu analogue, 4-α-phorbol. Although phorbol esters are known to cause activation of proteins other than PKC, such as chimaerin, Munc 13-1, Unc13, or Ras-GRP (Ron and Kazanietz, 1999), none of these proteins are kinases and therefore their activity should not be sensitive to ATP site-active PKC inhibitors such as Bis 1 used in this study. In contrast to activation, inhibition of PKC with Bis or related compounds was surprisingly without observable effects. This could indicate that a minimal level of basal PKC

activity is required for the maintenance of GC structure under the conditions employed here. This finding apparently contradicts the "growth-cone collapse" due to PKC inhibition after introduction of protein kinase C pseudosubstrate peptides reported earlier (Theodore et al., 1995). Indeed, we observed effects similar to "growth-cone collapse" when we tested inhibitors such as chelerythrine or calphostin C that interact with regions of PKC other than the C3 (ATP binding) domain (our unpublished observations). Caution should be exercised, however, in interpreting effects of these agents on growth cone structure, given that chelerythrine is reported to have direct effects on MT polymerization, and calphostin C has unpredictable phototoxic effects due to light-stimulated oxidative damage to PKC (Gopalakrishna et al., 1992; Wolff and Knipling, 1993). It has also been suggested that the regulatory domain of PKC, especially the pseudosubstrate, the C1 domain, and part of the V3 region, may be necessary and sufficient for sustaining neurite outgrowth (Zeidman et al., 1999). These observations are consistent with the aforementioned disruption of growth-cone structure after introduction of excessive pseudosubstrate peptide into growth cones (Theodore et al., 1995). The difference in the effects of ATP- and pseudosubstrate-based inhibitors may lie in the fact that addition of pseudosubstrate may increase availability of the regulatory domain for interactions while inhibiting the ATP transfer function of the kinase, whereas ATP-based inhibitors will only inhibit ATP transfer without affecting availability of the regulatory domain. It should be noted that our culture conditions (i.e., serum-free defined medium and poly-L-lysine substrate) minimize cross-talk between cell adhesion molecule and growth factor signaling pathways, which could have a significant effect upon the ultimate response of the neurons to PKC activation. These factors should be kept in mind when comparing the responses reported here to those observed in more complex systems.

MT Extension after PKC Activation Depends on Polymer Assembly

Previous studies on the effects of nocodazole in cells have demonstrated that concentrations in the 4–400-nM range inhibit MT dynamics without resulting in significant loss of MT polymer mass (Rochlin et al., 1996; Jordan and Wilson, 1998b; Jordan and Wilson, 1999). In the current study, similar treatments with extremely low doses of nocodazole and other inhibitors that interfere with MT polymerization potently inhibited PDBu-stimulated MT extension (Fig. 5), indicating that MT assembly is necessary for the effects reported here. Furthermore, our biochemical experiments showed an increase in MT polymer mass after PDBu treatment, and this MT polymer was also sensitive to depolymerization by low doses of nocodazole (Fig. 6). In support of the current findings in neurons, PDBu has also been reported to increase MT polymerization in macrophages (Robinson and Vandre, 1995).

To directly address the role of MT assembly, we measured MT dynamics using the FSM MT marking technique. This is a powerful new technique pioneered by Waterman-Storer and Salmon (1998) for investigating cytoskeletal protein dynamics in living cells, which enables independent assessment of the contribution of polymer as-

sembly dynamics and polymer translocation events. FSM analysis revealed that MT polymerization is indeed affected by PDBu treatment; specifically, the duration of typical MT assembly events were increased approximately twofold (Fig. 7, H and I). This increase in MT growth lifetimes was accompanied by a 1.7-fold decrease in catastrophe and approximately twofold increase in rescue frequencies (Table I). It should be noted that control rescue frequencies may be underestimated due to the difficulty in detecting rescue events occurring in relatively short MTs near the C–T-domain interface, where MT density is high (see Tanaka and Kirschner, 1991). To investigate this issue, a subpopulation of long MTs with ends already in the P-domain under control conditions were analyzed (Table I). In this population, the catastrophe frequency still decreased 1.7-fold in PDBu relative to controls; however, the rescue frequencies increased only ~1.3-fold. This smaller PDBu effect on peripheral (i.e., long) versus total MTs might result from inefficient detection of rescue events when assessed in the total MT population; however, we cannot rule out differences in MT behavior in the transition zone versus P-domain. These fundamental domain-specific issues are currently under investigation. Finally, actual rates of MT growth and shortening were not affected by PDBu (Table I), making changes in tubulin dimer concentration an unlikely mechanism for the observed MT advance.

Changes in rates of MT translocation are clearly not involved since retrograde and anterograde sliding rates were unaffected (Table I). In fact, the proportion of time MTs spent undergoing translocation in the retrograde direction was actually increased in PDBu (36% vs. 49% for control vs. PDBu, respectively) despite net MT advance. How can this paradox be resolved? Retrograde F-actin flow appears to act as a barrier to MT advance (Forscher and Smith, 1988), and retrograde translocation of MTs in peripheral F-actin domains has been described in nonneuronal cells (Waterman-Storer and Salmon, 1997). The current study supports these findings and suggests that when MTs extend into the P-domain, they do so predominantly by exhibiting prolonged bursts of assembly that exceed the rate of F-actin flow (e.g., Fig. 7 F). After extension, a MT can maintain its position in the P-domain by assembling at a rate that matches retrograde flow (e.g., Fig. 7 G); however, if MT assembly stops or slows below the rate of retrograde flow, the MT will be translocated rearward out of the P-domain. After PDBu treatment, the increased length of MTs within the P-domain promotes chances for MT-actin filament interactions, and this in turn may result in the increase in retrograde translocation events observed (Fig. 8 B). This scenario is consistent with the effects observed after stabilizing MTs with taxol; specifically, MTs were cleared from both the peripheral domain and transition zone, presumably via interactions with retrograde flow (Fig. 5 H). This explanation suggests a role for the actomyosin-based process (Lin et al., 1996) of retrograde F-actin flow in clearing MTs from the P-domain; however, it does not rule out participation of other molecular motors in the variety of MT translocation events observed (a detailed analysis of MT behavior in this system will be published separately).

Whether PDBu-stimulated MT advance results from direct effects on the MTs themselves, indirectly from alteration of F-actin structure, or from changes in MT–F-actin interactions remains to be determined. PDBu treatment does in fact affect F-actin structure; for example, in the inhibition of actin-based ruffling seen in Fig. 2 B. Several lines of evidence, however, suggest that the structure of the P-domain cytomatrix remains largely intact after PDBu treatment. First, the large (100–150-nm diameter) organelles typical of the C-domain do not significantly advance into the P-domain in PDBu. This is in contrast to treatment with cytochalasin, which disrupts peripheral F-actin and results in organelle advance into the P-domain (Forscher and Smith, 1988). Second, previous studies suggest that the P-domain pore size or gel exclusion limit is 70–100 nM (Popov and Poo, 1992), which is considerably larger than the ~25-nm diameter of a single MT, indicating that individual MTs would not be excluded from the P-domain simply on the basis of cross-sectional area alone. In agreement with this, we found that 2,000,000 kD FITC-dextran (~60-nm stokes radius) gained diffusional access into the P-domain and, furthermore, the distribution of this probe did not appear to change with PDBu treatment (our unpublished observations). Taken together, these observations suggest that organelles are simply sterically excluded from the peripheral domain by an F-actin–based barrier and the mechanism for MT exclusion from the P-domain is more complex.

What potential effector proteins might be involved? Recent evidence suggests the four parameters of MT dynamics (growth, shortening, catastrophe frequency, and rescue frequency) can be altered independently of one another in vivo (Desai and Mitchison, 1997; Andersen, 2000), so the situation is potentially complex. With that said, the current data does point to a mechanism involving modulation of the frequency of MT catastrophe and/or rescue events by PKC. Potential candidates are proteins that regulate MT catastrophe frequency such as Op18/stathmin (Belmont and Mitchison, 1996; Di Paolo et al., 1997), kinesin family members KIN 1 (Desai et al., 1999) and XKCM1 (Walczak et al., 1996; Tournebize et al., 2000), or XMAP310, a MT rescue-promoting factor (Andersen and Karsenti, 1997). On the other hand, phosphorylation of MAPs by PKC is well known to promote their dissociation from MTs, MT unbundling, and decreased MT stability (Mori et al., 1991; Gordon-Weeks, 1993; Goold et al., 1999), all of which are consistent with the results presented here. These lines of inquiry deserve further attention.

Implications of the Present Study

Previous analysis of PKC's regulation of neurite outgrowth have focused primarily on changes in F-actin structure and actin polymerization dynamics. Our findings suggest an additional mechanism for regulating the overall rate of axon growth through modulation of MT dynamics. PKC activation results in a net increase in MT polymerization via a pronounced increase in MT growth lifetimes, thus promoting MT extension into the P-domain. MT invasion of the P-domain could contribute to increased rates of neurite outgrowth we and many others have observed with chronic PKC activation (Hsu et al., 1989; Hundle et al., 1995; Fagerstrom et al., 1996). Interestingly, recent evidence suggests that dynamic MTs are necessary for delivery and incorporation of new membranes into the distal

axon (Zakharenko and Popov, 1998). Thus, PKC activation, by promoting MT growth, could also facilitate targeted delivery of membrane components.

References

Andersen, S.S. 2000. Spindle assembly and the art of regulating microtubule dynamics by MAPs and Stathmin/Op18. *Trends Cell Biol.* 10:261–267.

Andersen, S.S., and E. Karsenti. 1997. XMAP310: a *Xenopus* rescue-promoting factor localized to the mitotic spindle. *J. Cell Biol.* 139:975–983.

Bamburg, J.R., D. Bray, and K. Chapman. 1986. Assembly of microtubules at the tip of growing axons. *Nature.* 321:788–790.

Belmont, L.D., and T.J. Mitchison. 1996. Identification of a protein that interacts with tubulin dimers and increases the catastrophe rate of microtubules. *Cell.* 84:623–631.

Bixby, J.L. 1989. Protein kinase C is involved in laminin stimulation of neurite outgrowth. *Neuron.* 3:287–297.

Canman, J.C., and W.M. Bement. 1997. Microtubules suppress actomyosin-based cortical flow in *Xenopus* oocytes. *J. Cell Sci.* 110:1907–1917.

Challacombe, J.F., D.M. Snow, and P.C. Letourneau. 1997. Dynamic microtubule ends are required for growth cone turning to avoid an inhibitory guidance cue. *J. Neurosci.* 17:3085–3095.

Cramer, L.P., T.J. Mitchison, and J.A. Theriot. 1994. Actin-dependent motile forces and cell motility. *Curr. Opin. Cell Biol.* 6:82–86.

Dent, E.W., and K.F. Meiri. 1998. Distribution of phosphorylated GAP-43 (neuromodulin) in growth cones directly reflects growth cone behavior. *J. Neurobiol.* 35:287–299.

Desai, A., and T.J. Mitchison. 1997. Microtubule polymerization dynamics. *Annu. Rev. Cell. Dev. Biol.* 13:83–117.

Desai, A., S. Verma, T.J. Mitchison, and C.E. Walczak. 1999. Kin I kinesins are microtubule-destabilizing enzymes. *Cell.* 96:69–78.

Di Paolo, G., R. Lutjens, A. Osen-Sand, A. Sobel, S. Catsicas, and G. Grenningloh. 1997. Differential distribution of stathmin and SCG10 in developing neurons in culture. *J. Neurosci. Res.* 50:1000–1009.

Fagerstrom, S., S. Pahlman, C. Gestblom, and E. Nanberg. 1996. Protein kinase C-epsilon is implicated in neurite outgrowth in differentiating human neuroblastoma cells. *Cell Growth Differ.* 7:775–785.

Forscher, P., L.K. Kaczmarek, J.A. Buchanan, and S.J. Smith. 1987. Cyclic AMP induces changes in distribution and transport of organelles within growth cones of Aplysia bag cell neurons. *J. Neurosci.* 7:3600–3611.

Forscher, P., and S.J. Smith. 1988. Actions of cytochalasins on the organization of actin filaments and microtubules in a neuronal growth cone. *J. Cell Biol.* 107:1505–1516.

Goold, R.G., R. Owen, and P.R. Gordon-Weeks. 1999. Glycogen synthase kinase 3beta phosphorylation of microtubule-associated protein 1B regulates the stability of microtubules in growth cones. *J. Cell Sci.* 112:3373–3384.

Gopalakrishna, R., Z.H. Chen, and U. Gundimeda. 1992. Irreversible oxidative inactivation of protein kinase C by photosensitive inhibitor calphostin C. *FEBS Lett.* 314:149–154.

Gordon-Weeks, P.R. 1993. Organization of microtubules in axonal growth cones: a role for microtubule-associated protein MAP 1B. *J. Neurocytol.* 22:717–725.

Hartwig, J.H., M. Thelen, A. Rosen, P.A. Janmey, A.C. Nairn, and A. Aderem. 1992. MARCKS is an actin filament crosslinking protein regulated by protein kinase C and calcium-calmodulin. *Nature.* 356:618–622.

He, Q., E.W. Dent, and K.F. Meiri. 1997. Modulation of actin filament behavior by GAP-43 (neuromodulin) is dependent on the phosphorylation status of serine 41, the protein kinase C site. *J. Neurosci.* 17:3515–3524.

Hsu, L., A.Y. Jeng, and K.Y. Chen. 1989. Induction of neurite outgrowth from chick embryonic ganglia explants by activators of protein kinase C. *Neurosci. Lett.* 99:257–262.

Hundle, B., T. McMahon, J. Dadgar, and R.O. Messing. 1995. Overexpression of epsilon-protein kinase C enhances nerve growth factor-induced phosphorylation of mitogen-activated protein kinases and neurite outgrowth. *J. Biol. Chem.* 270:30134–30140.

Jordan, M.A., D. Thrower, and L. Wilson. 1992. Effects of vinblastine, podophyllotoxin and nocodazole on mitotic spindles. Implications for the role of microtubule dynamics in mitosis. *J. Cell Sci.* 102:401–416.

Jordan, M.A., and L. Wilson. 1998a. Microtubules and actin filaments: dynamic targets for cancer chemotherapy. *Curr. Opin. Cell Biol.* 10:123–130.

Jordan, M.A., and L. Wilson. 1998b. Use of drugs to study role of microtubule assembly dynamics in living cells. *Methods Enzymol.* 298:252–276.

Jordan, M.A., and L. Wilson. 1999. The use and action of drugs in analyzing mitosis. *Methods Cell Biol.* 61:267–295.

Letourneau, P.C. 1996. The cytoskeleton in nerve growth cone motility and ax-
onal pathfinding. *Perspect. Dev. Neurobiol.* 4:111–123.

Letourneau, P.C., T.A. Shattuck, and A.H. Ressler. 1987. "Pull" and "push" in neurite elongation: observations on the effects of different concentrations of cytochalasin B and taxol. *Cell Motil. Cytoskelet.* 8:193–209.

Lin, C.H., E.M. Espreafico, M.S. Mooseker, and P. Forscher. 1996. Myosin drives retrograde F-actin flow in neuronal growth cones. *Neuron.* 16:769–782.

Lin, C.H., and P. Forscher. 1995. Growth cone advance is inversely proportional to retrograde F-actin flow. *Neuron.* 14:763–771.

Lin, C.H., C.A. Thompson, and P. Forscher. 1994. Cytoskeletal reorganization underlying growth cone motility [published erratum appears in *Curr. Opin. Neurobiol.* 1995. 5:112]. *Curr. Opin. Neurobiol.* 4:640–647.

Liu, C.W., G. Lee, and D.G. Jay. 1999. Tau is required for neurite outgrowth and growth cone motility of chick sensory neurons. *Cell Motil. Cytoskelet.* 43:232–242.

Meiri, K.F., M. Willard, and M.I. Johnson. 1988. Distribution and phosphorylation of the growth-associated protein GAP-43 in regenerating sympathetic neurons in culture. *J. Neurosci.* 8:2571–2581.

Mitchison, T., and M. Kirschner. 1988. Cytoskeletal dynamics and nerve growth. *Neuron.* 1:761–772.

Mitchison, T.J., and L.P. Cramer. 1996. Actin-based cell motility and cell locomotion. *Cell.* 84:371–379.

Mori, A., H. Aizawa, T.C. Saido, H. Kawasaki, K. Mizuno, H. Murofushi, K. Suzuki, and H. Sakai. 1991. Site-specific phosphorylation by protein kinase C inhibits assembly-promoting activity of microtubule-associated protein 4. *Biochemistry.* 30:9341–9346.

Nakhost, A., P. Forscher, and W.S. Sossin. 1998. Binding of protein kinase C isoforms to actin in Aplysia. *J. Neurochem.* 71:1221–1231.

Popov, S., and M.M. Poo. 1992. Diffusional transport of macromolecules in developing nerve processes. *J. Neurosci.* 12:77–85.

Robinson, J.M., and D.D. Vandre. 1995. Stimulus-dependent alterations in macrophage microtubules: increased tubulin polymerization and detyrosination. *J. Cell Sci.* 108:645–655.

Rochlin, M.W., K.M. Wickline, and P.C. Bridgman. 1996. Microtubule stability decreases axon elongation but not axoplasm production. *J. Neurosci.* 16:3236–3246.

Ron, D., and M.G. Kazanietz. 1999. New insights into the regulation of protein kinase C and novel phorbol ester receptors. *FASEB J.* 13:1658–1676.

Rosner, H., and H. Fischer. 1996. In growth cones of rat cerebral neurons and human neuroblastoma cells, activation of protein kinase C causes a shift from filopodial to lamellipodial actin dynamics. *Neurosci. Lett.* 219:175–178.

Sossin, W.S., and J.H. Schwartz. 1994. Translocation of protein kinase Cs in Aplysia neurons: evidence for complex regulation. *Brain Res. Mol. Brain Res.* 24:210–218.

Suter, D.M., L.D. Errante, V. Belotserkovsky, and P. Forscher. 1998. The Ig superfamily cell adhesion molecule, apCAM, mediates growth cone steering by substrate-cytoskeletal coupling. *J. Cell Biol.* 141:227–240.

Tanaka, E., T. Ho, and M.W. Kirschner. 1995. The role of microtubule dynamics in growth cone motility and axonal growth. *J. Cell Biol.* 128:139–155.

Tanaka, E., and J. Sabry. 1995. Making the connection: cytoskeletal rearrangements during growth cone guidance. *Cell.* 83:171–176.

Tanaka, E.M., and M.W. Kirschner. 1991. Microtubule behavior in the growth cones of living neurons during axon elongation. *J. Cell Biol.* 115:345–363.

Theodore, L., D. Derossi, G. Chassaing, B. Llirbat, M. Kubes, P. Jordan, H. Chneiweiss, P. Godement, and A. Prochiantz. 1995. Intraneuronal delivery of protein kinase C pseudosubstrate leads to growth cone collapse. *J. Neurosci.* 15:7158–7167.

Tournebize, R., A. Popov, K. Kinoshita, A.J. Ashford, S. Rybina, A. Pozniakovsky, T.U. Mayer, C.E. Walczak, E. Karsenti, and A.A. Hyman. 2000. Control of microtubule dynamics by the antagonistic activities of XMAP215 and XKCM1 in *Xenopus* egg extracts. *Nat. Cell Biol.* 2:13–19.

Walczak, C.E., T.J. Mitchison, and A. Desai. 1996. XKCM1: a *Xenopus* kinesin-related protein that regulates microtubule dynamics during mitotic spindle assembly. *Cell.* 84:37–47.

Waterman-Storer, C.M. 1998. Microtubules and microscopes: how the development of light microscopic imaging technologies has contributed to discoveries about microtubule dynamics in living cells. *Mol. Biol. Cell.* 9:3263–3271.

Waterman-Storer, C.M., A. Desai, J.C. Bulinski, and E.D. Salmon. 1998. Fluorescent speckle microscopy, a method to visualize the dynamics of protein assemblies in living cells. *Curr. Biol.* 8:1227–1230.

Waterman-Storer, C.M., and E.D. Salmon. 1997. Actomyosin-based retrograde flow of microtubules in the lamella of migrating epithelial cells influences microtubule dynamic instability and turnover and is associated with microtubule breakage and treadmilling. *J. Cell Biol.* 139:417–434.

Waterman-Storer, C.M., and E.D. Salmon. 1998. How microtubules get fluorescent speckles. *Biophys. J.* 75:2059–2069.

Wolff, J., and L. Knipling. 1993. Antimicrotubule properties of benzophenanthridine alkaloids. *Biochemistry.* 32:13334–13339.

Zakharenko, S., and S. Popov. 1998. Dynamics of axonal microtubules regulate the topology of new membrane insertion into the growing neurites. *J. Cell Biol.* 143:1077–1086.

Zeidman, R., B. Lofgren, S. Pahlman, and C. Larsson. 1999. PKCepsilon, via its regulatory domain and independently of its catalytic domain, induces neurite-like processes in neuroblastoma cells. *J. Cell Biol.* 145:713–726.